A Steerable Dual-Channel Microwave Radiometer for Measurement of Water Vapor and Liquid in the Troposphere

D. C. HOGG, F. O. GUIRAUD, J. B. SNIDER, M. T. DECKER AND E. R. WESTWATER

NOAA/ERL/Wave Propagation Laboratory, Boulder, CO 80303

(Manuscript received 9 September 1982)

ABSTRACT

An instrument that remotely senses the integrated amounts of water vapor and liquid on a path through the atmosphere is discussed. The vapor and liquid are measured simultaneously but independently by microwave radiometers. Comparison of the accuracy in measurement of vapor is made with radiosondes, and of liquid with an independent method employing transmission from a geosynchronous satellite. The instrument is designed for unattended operation; examples of measured data are given. Applications including observations for weather forecasting, weather modification, solar-radiation studies, and instrumentation for geodetic metrology are also discussed.

1. Introduction

The amount of tropospheric water vapor and liquid is highly variable in both time and space, therefore continuous measurements in real time are needed to determine the evolution of these quantities. Examples of applications of such data are encountered in determining heat balance in climatology, in weather-modification experiments and in forecasting on the mesoscale. At microwave wavelengths, both water vapor and liquid possess absorptive properties, and therefore produce emission that is detected by radiometers. The emission "signals" are then processed by a suitable algorithm to retrieve the integrated amounts of vapor and liquid in the beam of the radiometric antenna. For versatility, the beam must be fully steerable.

Application of a 20–30 GHz microwave radiometer (Guiraud *et al.*, 1979) to measurement of water vapor has shown that the accuracy in measurement of precipitable water vapor is better than that of operational radiosondes (see also Hogg *et al.*, 1983, in a companion paper, this issue). Radiometric measurement of the integrated amount of liquid, when liquid-bearing clouds are in the antenna beam, cannot be compared with operational radiosondes since the latter do not make measurements of liquid routinely. However, a separate and independent instrument for accurate measurement of cloud liquid, based on transmission methods (Snider *et al.*, 1980a), has been used for direct comparison with dual-channel radiometry (Snider *et al.*, 1980b). These comparisons show that dual-channel radiometers indeed provide accurate values for the amount of integrated liquid in clouds.

Because ice has negligible absorption at these frequencies and therefore has negligible emission, ice clouds and dry snow are not detected by this instrument.

The vapor and liquid are measured simultaneously and also independently, provided the liquid content is not too high, e.g., during heavy rain.

2. Factors influencing design of the instrument

Seven design considerations that result in high stability, sensitivity, and reliability in the instrument are discussed in detail in the following sections; they are:

- Two frequencies, 20.6 and 31.6 GHz, are used, affording simultaneous measurement of the integrated vapor and the liquid in clouds (Sections 3, 8 and 10).
- The frequency, 20.6 GHz, which primarily senses the vapor, is removed from the peak of the absorption line (22.2 GHz); this results in a measurement of integrated vapor that is relatively independent of pressure, (Westwater, 1967), i.e., independent of the particular distribution of water vapor with height (Sections 3, 8 and 9).
- 31.6 GHz primarily senses the liquid (Sections 3 and 8).
- The electronics of the radiometer, the antenna and associated feed are all housed in a benign environment (Section 4).
- The antenna system, an offset paraboloid with a hybrid-mode feed and flat reflectors for beam steering results in high-quality radiation patterns that minimize the effect of extraneous sources of radiation

(noise); the antenna aperture is devoid of blockage (Section 4); all-weather operation is a major principle guiding the design and fabrication.

- The antenna operates with the same beamwidth at the two frequencies; this allows for proper operation when liquid-bearing clouds are present, i.e., with the same filling of the beams, and also leads to high accuracy in measurement of vapor at low elevation angles.
- The radiometer is triple-switched, two reference loads being provided; this results in continuous unattended calibration and high stability.

3. Frequency considerations

It is common practice to use a frequency at the peak of an absorption line to measure the amount or density of a substance. In particular, when radiometric techniques are used, the "signal-to-noise" ratio is largest at that frequency; provided the pressure and temperature are constant, using this frequency can result in a good measure of the amount of the substance.

But when the pressure and temperature change, as occurs with height for water vapor in the troposphere, operation at the line center is not optimal. The physical reasoning behind this argument is indicated schematically in Fig. 1 by the pressure-broadening of the absorption line at 22.2 GHz. As indicated, at 20.6 GHz the change in absorption caused by pressure broadening is minimized but at the expense of dropping to about three-quarters of the peak absorption. Calculations on the improvement in accuracy of determining atmospheric vapor using 20.6 GHz (rather than 22.2 GHz), calculated from typical profiles measured by radiosondes, are given by Westwater (1978).

The other frequency in the dual-channel system, 31.65 GHz, is situated in a transmission "window" of the troposphere. At this frequency, the absorption coefficient of water vapor under standard conditions is lower than the value at 20.6 GHz by a factor of about 1.8. Conversely, absorption by liquid water at

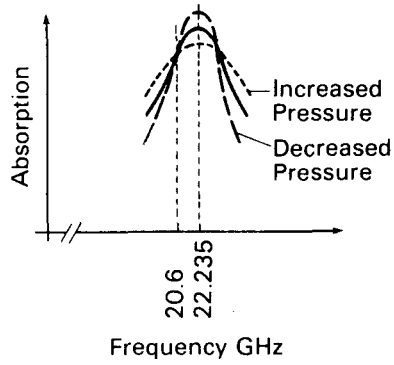

FIG. 1. Absorption by water vapor at different pressures showing variation on the peak of the line and invariance at 20.6 GHz.

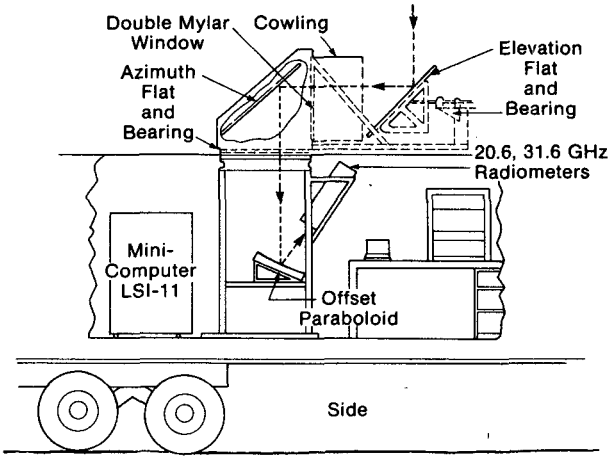

FIG. 2. Side view of a steerable dual-channel radiometer showing the mechanical layout; a central ray from the zenith is shown as dashed lines with arrows.

31.65 GHz is about 2.2 times greater than that at 20.6 GHz. From an operational point of view, 31.65 GHz is desirable because it is centered in a band allocated to passive space research.

The brightness temperatures at the two frequencies are incorporated in a pair of simultaneous equations to retrieve the amounts of vapor and liquid. In Section 8, the method of retrieval and the coefficients in these equations are discussed in more detail.

4. Physical configuration

A cross-section of the physical layout of the system is shown in Fig. 2. The electronics for both the 20.6 and 31.6 GHz radiometers are located in a single package, and the feed horn for the offset paraboloid is mounted in a wall of the box containing the electronics. This arrangement provides a benign environment, in particular essentially constant temperature, for both the electronics and the antenna. The minicomputer, an LSI 11/02, is also located inside the trailer. A heat pump (not shown) is used to stabilize the temperature of the trailer housing.

The offset paraboloid and feed horn are of the same design as discussed by Hogg *et al.* (1979); the configuration is such that the aperture is unblocked and the corrugated (multi-mode) feed such that equal beamwidths are produced at 20.6 and 31.6 GHz. The performance of this feed-reflector combination is discussed in detail in the above reference. It remains to provide full steerability for the beam without introducing blockage to the radiation.

The roof of the trailer, although structurally strong, is further braced by supports surrounding the offset paraboloid as indicated in Fig. 2. Above these supports is incorporated a bearing which is 75 cm in diameter. On this bearing, in turn, is mounted a structure (rotatable with the bearing) that serves as a sup-

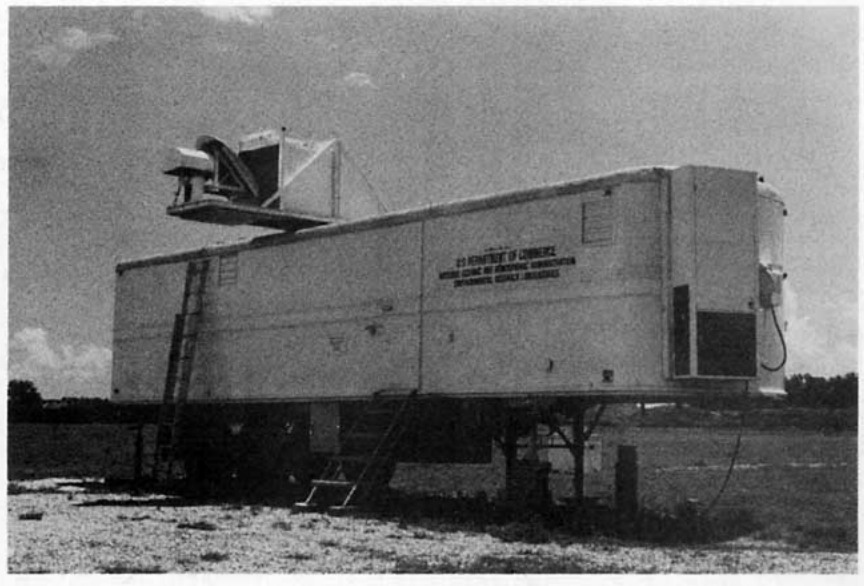

FIG. 3. Side view of a mobile dual-channel radiometer located at the Denver Weather Service Forecast Office.

port for two flat reflectors. The flat immediately above the bearing is fixed on the rotatable structure; it is referred to as the azimuth flat in Fig. 2. The flat on the outrigger of the structure is mounted on an independent bearing that rotates in a plane orthogonal to the azimuth bearing. When this flat is rotated, the antenna beam scans in elevation; it is referred to as the elevation reflector in Fig. 2. Full-sky coverage by the antenna beam can therefore be achieved by suitable rotation of the two bearings (modes of scan are discussed further in later sections). External elements of the antenna system are shown on top of the trailer in Fig. 3.

The azimuth flat and bearing are protected with a weather-tight cover fitted with a multilayer microwave window (see Fig. 2). The window is formed of mylar sheets 0.05 mm thick; it is shielded from the weather by a cowling whose primary function is to prevent rain from wetting the microwave window. A double window is used to help prevent condensation on the outer surface during humid conditions. An external heater on the floor of the cowling is added if condensation is a factor. The physical rationale for this design is that, in the case of the reflector, radiation reflects (in part) from a water layer, whereas if a wetted window were involved, the radiation must pass through. For a layer thickness of 0.1 mm, for example, the wet window absorbs about 50 times more than the wet reflector, and the brightness temperature is about 30 times higher.

Mobility of the instrument is achieved by using a trailer as both a small laboratory and an antenna platform. However, because of clearance restrictions on many highways, the flat-reflector assembly is removed from the azimuth bearing and stored in the trailer for long-distance transport. Several long-distance trips have been satisfactory in every respect.

5. Electronics package and computer

The radiometers are of the Dicke switching type and are operating in an off-balance mode. Both radiometers, including all associated electronics, are mounted in the same 46 × 18 × 61 (cm) enclosure. The power supplies and controls are excluded from the package for convenience and because of temperature considerations. Table 1 lists the characteristics of the radiometers. We apply signal integration external to the radiometers, which improves the sensitivity further.

The radiometer design can best be understood by following the block diagram, Fig. 4. Emission signals are focused into a wideband feed by an offset 50 cm × 50 cm paraboloidal surface (not shown in the block diagram). Following the antenna feed, the two frequencies are split and passed to the two radiometers. The through port of the splitter is stepped down in size to the 31.65 GHz waveguide, and the 20.6 GHz signal is taken from the sidewall port. The switch is a three junction, five-port, ferrite device; it requires slightly over one microsecond to settle after being switched and can be toggled at a 2 kHz rate. The design of the radiometers extends the normal Dicke design by adding a second calibration source to the switching sequence (Guiraud *et al.*, 1979). The source we refer to as the reference load is a temperature controlled, waveguide termination; the temperature

TABLE 1. Radiometer characteristics.

	Radiometer 1	Radiometer 2
Center frequency	20.6 GHz	31.6 GHz
Bandwidth	1 GHz	1 GHz
Receiver noise temperature	680 K	725 K
Sensitivity w AGC	0.26 K	0.26 K

is controlled at 45°C, a level higher than the expected ambient will reach. The second source, the "hot load," is also a temperature controlled waveguide termination at 145°C. Junctions A and B are used to connect in sequence the antenna, the hot load and the reference loads to the mixer through Junction C.

The microwave mixers are of balanced design, using selected low noise Schottky-barrier diodes. Incorporated in the mixer package is a series of thin-film wideband amplifiers with a video detector at the output. A 50 MHz high-pass filter is added in the IF section to reduce shot noise; to maximize sensitivity no other filtering is added. The high side of the band pass of the amplifiers exceeds 1.5 GHz. Sufficient gain is provided by an external video amplifier to produce a 2 volt peak-to-peak video signal at the input to the synchronous detectors. Two synchronous detectors are required to make use of the triple switching. One is gated to detect the power difference between the antenna and reference load; the other to detect the difference between the reference and the hot load. The voltage produced by the second synchronous detector is in effect a monitor of any changes in gain and is used as an automatic-gain-control (agc) level in the computer. The output from the first synchronous detector is referred to as the signal channel. The synchronizing oscillator controls the switching sequence of the ferrite switch and the gating of the synchronous detectors.

The dotted lines surrounding areas in the block diagram (Fig. 4), are areas under temperature control; thermistors are used as the temperature-sensing elements. The hot load and reference load are temperature controlled, and we also include the ferrite switch block with the reference load; this ensures that the associated waveguide losses of the switch do not modify our reference noise level. A 0.1°C temperature control for the reference load and hot load is maintained for weeks on end. The whole electronic package is temperature stabilized near 37°C. Linearized thermistors are used to monitor the temperatures of the hot load, reference load, and antenna waveguide; these measurements are all critical to accurate reduction of the brightness measurements.

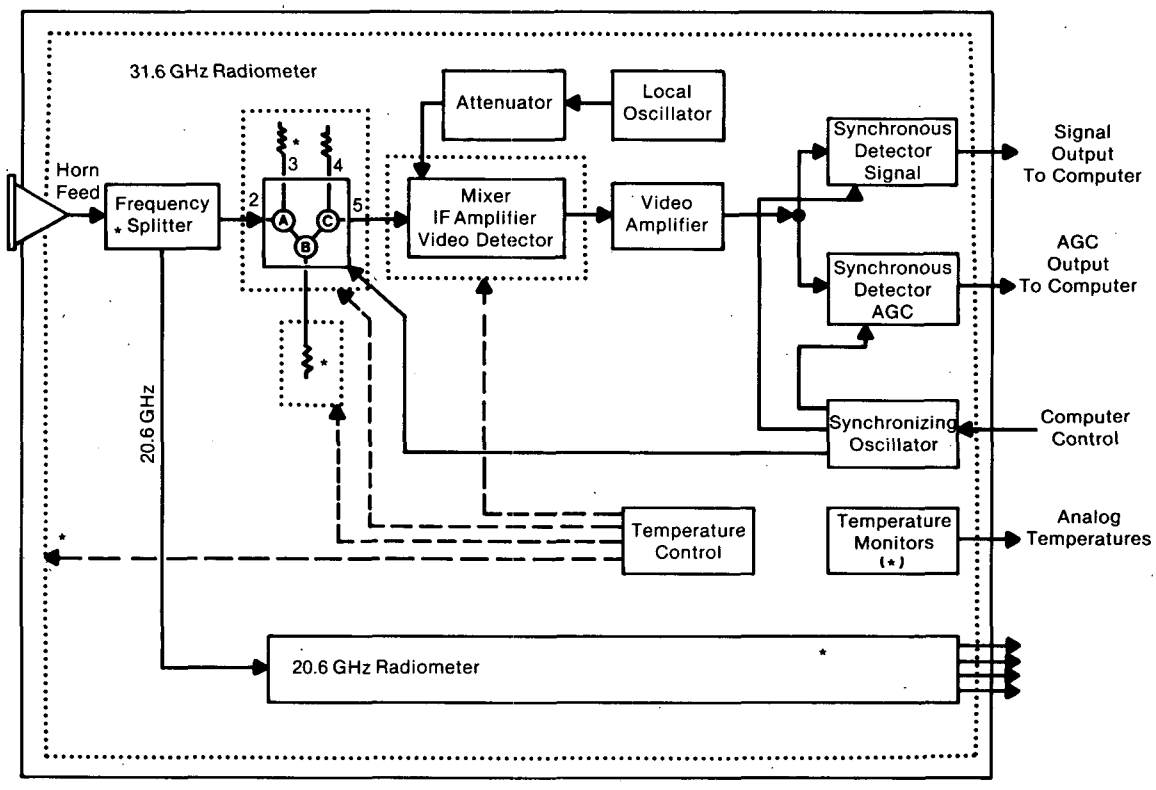

FIG. 4. Electrical layout of a radiometer; temperature is monitored at points marked by asterisks.

6. Computer system

Data from the dual-channel radiometer are processed in real-time in an LSI-11/02 minicomputer. In addition, the computer system controls many radiometer functions including data sampling rates, averaging intervals, output data rates and initiation of periodic radiometer self-calibrations. In the present model, antenna position is not controlled by the computer; however, this capability can be readily added if desired.

The LSI-11/02 minicomputer operates with 32 000 16-bit words of active semiconductor memory; inactive system software and radiometer data are stored on magnetic disks. The magnetic disk drive unit contains both a fixed and a removable disk. Each disk has two recording surfaces with a storage capacity of 4762 512-word blocks. System software is stored on the fixed disk and radiometric data are archived on the removable disk.

Communication with the computer is through a teletype terminal. Output data are also printed out periodically on the terminal.

Computer software supports three radiometer modes of operation:

1) Fixed azimuth and elevation angles,
2) Continuous 360 degree azimuth scans at a fixed elevation angle,
3) Variable azimuth or elevation scans with the remaining axis fixed.

The system is capable of unattended, continuous operation in modes 1 and 3. Mode 2, which is employed to measure the spatial distribution of vapor and liquid in clouds, requires an operator to be present. Operating mode is changed either by activating the appropriate computer program or, for mode 2, by modifying the input parameters to a single program. In all modes, the start of operation is self-prompting, i.e., the operator enters input parameters into the teletype terminal in response to questions from the computer. Thereafter, program execution is continuous until stopped by the operator.

Processed data outputs, path-integrated water vapor and path-integrated liquid, are continuously displayed on a two-channel strip-chart recorder. The recorder display is scaled to indicate directly total water vapor in cm and total liquid in mm. In addition, the output data are printed on the computer teletype at certain intervals. The print-out also includes a simple plot of water vapor and total liquid versus time for ready identification of trends. Unprocessed radiometric data are written on a removable magnetic disk for later processing if desired. Table 2 summarizes the sample rates, input data averaging times and output data update intervals for the three operating modes. Output data are averaged over the intervals shown.

TABLE 2. Summary of data-processing characteristics for steerable dual-channel radiometer.

Mode of operation	Sample rate (Hz)	Averaging time (s)	Output interval		
			Strip-chart	Printer*	Disk
1	10	10	10 s	10 min	2 min
2	10	1	1 s	5 min	5 s
3	10	1	1 s	2.5 deg	2.5 deg

* A print-on-demand feature offers printouts at 2 min, 5 s and 15 s intervals, for modes 1, 2, and 3, respectively.

A 1.0-s radiometer time constant is used in all modes of operation. In order to ensure an adequate number of independent samples within the nominal antenna beamwidth of 2.5 degrees, the antenna scan rate is limited to 0.5 deg s^{-1}. At the maximum scan rate, five 1-s samples are obtained in 2.5 degrees of antenna rotation.

7. Calibration

The two temperature controlled loads discussed in Section 5a are used to establish the relationship between voltage output from the radiometers and input brightness; junction B in Fig. 4 is the first common point for all the signals. Since the waveguide leading to the reference load is at the same temperature as the reference load, the emission generated by the guide exactly compensates for the quantity attenuated; this is not the case for the signals coming from the antenna and hot load. For the transmission path to the antenna we first estimate the attenuation because it is extremely difficult to make a direct measurement of such low attenuation. By monitoring the physical temperature of the antenna line, we account for both added emission and attenuation effects on the signal. The waveguide from the hot load is temperature controlled either in the hot load or in the ferrite switch; the emission is therefore unchanging, and we identify a factor with which we can multiply the indicated hot load temperature to determine its effective temperature at junction B.

A value for this factor is found from a series of "tipping curve" or elevation-scan measurements made on cloudless days when the emission from the atmosphere is unchanging. An initial calibration is made by first placing a high quality absorber in front of the antenna; the output voltage from the radiometers and the physical temperature of the absorber are noted. The antenna is then directed toward the zenith, and the output voltage is again noted. The zenith brightness temperatures may fall between 10 and 40 K depending on the amount of vapor present; initially a value of 20 K can be assumed. Using this assumption and knowing the temperature of the absorber, the two points are used to define a temporary

calibration. These tropospheric emission measurements are related to absorption (τ) by the expression

$$\tau = \ln(T_m - 2.9)/(T_m - T_b), \quad (1)$$

where the absorption is in nepers,[1] T_m is the mean radiating temperature for the atmosphere, T_b the brightness at the antenna input, and 2.9 is a constant representing the cosmic background, all in K.

For calibration purposes, a relative value of absorption is all that is needed. The temperature T_m is estimated at 270 K. We now plot the absorption measurements taken by scanning in elevation, against the number of atmospheres (secant of the zenith angle). This curve is linear and must pass through the origin, secant equal to zero, i.e., no atmosphere—no absorption. The plot is adjusted to force it through zero, if the assumption made in the initial two-point calibration is not correct. The value of the adjusted curve at one air mass is then the true relative zenith absorption. Typical tipping curves showing measurements of absorption at both frequencies versus number of atmospheres are given in Fig. 5. The true zenith brightness is found by solving (1) for T_b. In turn, the hot load multiplying factor is found, thus establishing an absolute calibration for the radiometers.

8. Retrieval methods

a. Statistical inversion

In deriving total precipitable water vapor and integrated cloud liquid from radiometric observations, statistical retrieval methods are commonly employed (Guiraud *et al.*, 1979; Westwater and Guiraud, 1980; Grody *et al.*, 1980; Staelin *et al.*, 1976). We will outline this method below, first in a form that is appropriate in the case where nonprecipitating clouds with low attenuation are involved, and then in an adaptive form that is designed to treat relatively high attenuation due to clouds bearing a considerable amount of liquid water.

Under conditions of low attenuation, total absorption can be derived from atmospheric emission (Hogg and Chu, 1975). This absorption can, in turn, be directly related to corresponding amounts of integrated water vapor V and cloud liquid L. As discussed by Staelin (1966) measurements of low attenuation at a vapor-sensitive frequency and a liquid-sensitive frequency allow separation of the two phases.

If the total atmospheric transmission at frequency ν is written as $\exp(-\tau_\nu)$, then measurements of microwave brightness temperature $T_{b\nu}$ can be converted to absorption τ_ν by

$$\tau_\nu = -\ln[(T_{mr} - T_{b\nu})/(T_{mr} - T_{bb})], \quad (2)$$

as in (1), where T_{bb} is the cosmic background brightness temperature taken to be 2.9 K, and T_{mr} is an estimated "mean radiating temperature." For nonprecipitating clouds, we can write

$$\tau_\nu = \kappa_{V\nu}V + \kappa_{L\nu}L + \tau_{d\nu}, \quad (3)$$

where $\kappa_{V\nu}$ and $\kappa_{L\nu}$ are path-averaged mass absorption coefficients of vapor and liquid, and $\tau_{d\nu}$ is the dry absorption. Since microwaves radiate only very weakly from ice clouds (Staelin *et al.*, 1975), their effect is neglected here.

In the usual experimental situation neither the mass absorption coefficients $\kappa_{V\nu}$ and $\kappa_{L\nu}$ nor the dry absorption $\tau_{d\nu}$ are known since they depend on the unknown spatial distributions of pressure, temperature and humidity. As an example, Table 3 shows calculations of the climatological variation of these quantities over a two-month period at Oklahoma City, Oklahoma. Note, in particular, that the liquid-attenuation coefficients are subject to variations of the order of 25–30%. Because of this variation, deriving V and L from dual-frequency measurements by simple matrix inversion is not optimal, and we use instead statistical inversion. The application of this technique to ground-based microwave remote sensing is thoroughly discussed by Decker *et al.* (1978). For completeness we briefly outline the method below.

The linear statistical inversion algorithm may be written (Deutsch, 1965) as

$$\hat{\mathbf{p}} = \langle \mathbf{p} \rangle + \langle \mathbf{p}'\mathbf{d}'^{\mathrm{T}} \rangle \langle \mathbf{d}'\mathbf{d}'^{\mathrm{T}} \rangle^{-1} \mathbf{d}', \quad (4)$$

where $\hat{\mathbf{p}}$ is the estimate of the vector $\mathbf{p}$, $\mathbf{d}$ is the data vector, $\langle \cdot \rangle$ refers to ensemble average, $\mathbf{d}^{\mathrm{T}}$ is the transpose of the vector $\mathbf{d}$, and the primed quantities refer to departures from the average, i.e., $\mathbf{d}' = \mathbf{d} - \langle \mathbf{d} \rangle$. The matrix inverse $\langle \mathbf{d}'\mathbf{d}'^{\mathrm{T}} \rangle^{-1}$ is assumed to exist.

In our applications of (4) to determine V and L from measurements of brightness temperature $T_{b\nu}$, the two-component data vector $\mathbf{d}$ is chosen to be the total absorption τ_ν, ν = 20.6 GHz, 31.65 GHz. In using (2), the quantity τ_ν is derived from $T_{b\nu}$ and a climatological average mean radiating temperature. The ensemble over which the averages and covariances in (4) are calculated is based on a history of radiosonde profiles; clouds are inserted into this ensemble following the modeling scheme described by Decker *et al.* (1978). Brightness temperatures are calculated from the radiosondes using a standard water-vapor absorption model (Waters, 1976) which accounts for the empirical excess attenuation related to the continuum absorption (Deepak, 1980; Gaut and Reifenstein, 1971; Hogg, 1959);[2] instrument noise is

[1] The number of nepers is given by the natural logarithm of the ratio of output to input power transmitted through an absorbing medium.

[2] Evidence is beginning to mount that the dependence of this absorption on total and partial pressure is considerably nonlinear; this may lead to some modification of the absorption coefficients.

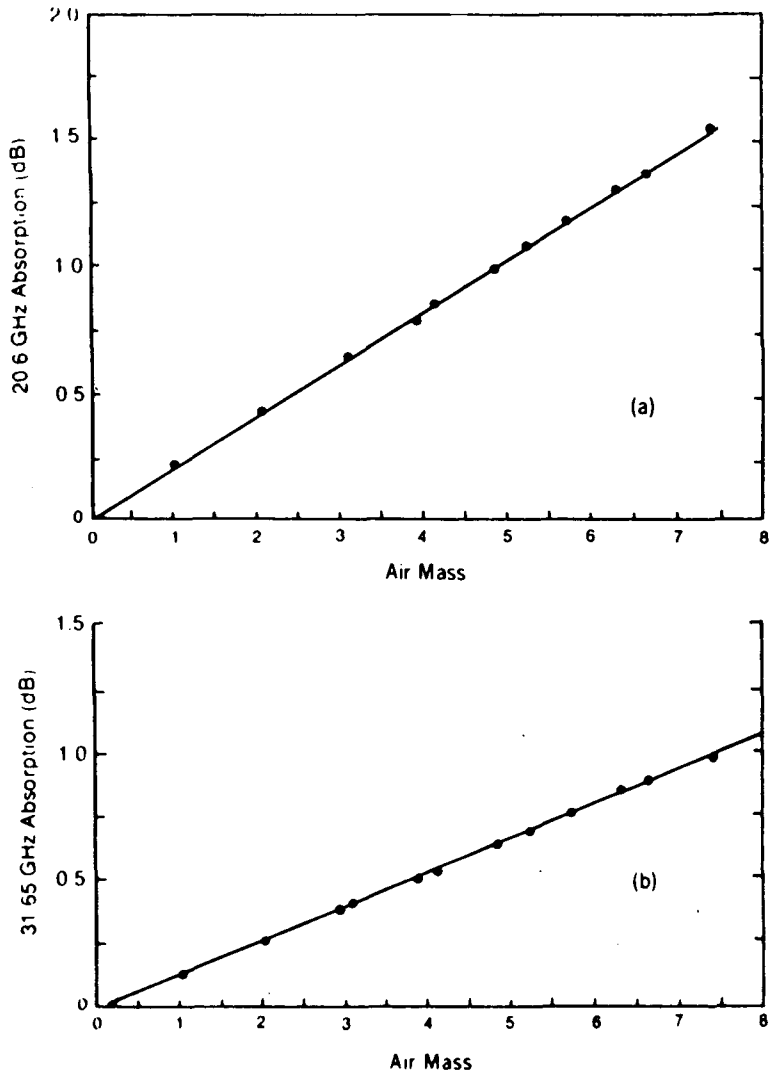

FIG. 5. Measured absorption at (a) 20.6 GHz and (b) 31.65 GHz versus air mass on a clear day at Denver, Colorado; these tipping curves are used in initial calibration of the instrument.

simulated by assuming Gaussian noise. Numerical values of the coefficients in (4) for selected climatologies are given in Table 4a for vapor and in Table 4b for liquid. For these tables, the optical depth τ is in nepers, and an instrumental noise level of 1.0 K is assumed. In essence, (4) leads to the solution of two equations with two unknowns.

The predicted rms accuracies in the radiometric

TABLE 3. Climatological variation of parameters used in deriving vapor and liquid from dual-channel radiometric observations. Based on Oklahoma City radiosonde observations during April–May 1975–77. ν_l = 20.6 GHz, ν_u = 31.65 GHz.

	τ_{dl} (Np)*	τ_{du} (Np)	κ_{Vl} (Np per cm H_2O)	κ_{Vu} (Np per cm H_2O)	κ_{Ll} (Np per cm H_2O)	κ_{Lu} (Np per cm H_2O)	$\frac{\kappa_{Vl}}{\kappa_{Vu}}$	$\frac{\kappa_{Lu}}{\kappa_{Ll}}$	$T_{mr,l}$ (K)	$T_{mr,u}$ (K)
Average	0.01320	0.02336	0.04257	0.02417	0.8289	1.7761	1.7761	2.2538	277.8	275.4
Standard deviation	0.00033	0.00059	0.00034	0.00127	0.2423	0.4978	0.0926	0.0492	5.1	5.7
$\frac{\text{Standard deviation}}{\text{Average}} \times 100$	2.51	2.51	0.79%	5.26%	29.23%	26.81%	5.25%	2.18%	1.8%	2.1%

* See footnote 1 p 794 for definition.

TABLE 4. Numerical values of the coefficients in Eq. (4).

(a) Water vapor

$\hat{V} = a_0 + a_{20.6} \cdot \tau_{20.6} + a_{31.65} \cdot \tau_{31.65}$ (cm)

	a_0	$a_{20.6}$	$a_{31.65}$	T_{mr} (K) 20.6 GHz	T_{mr} (K) 31.65 GHz
Sterling VA Jul–Nov	−0.05662	30.429	−12.754	281.04	279.90
Sheridan CA Nov–Apr	−0.03980	30.408	−13.363	272.99	271.13
Oklahoma City OK Apr–May	−0.02067	29.623	−12.593	277.8	275.4
Denver CO All Year	−0.00111	26.966	−11.772	268.49	265.47

(b) Liquid

$\hat{L} = b_0 + b_{20.6} \cdot \tau_{20.6} + b_{31.65} \cdot \tau_{31.65}$ (cm)

	b_0	$b_{20.6}$	$b_{31.65}$
Sterling VA Jul–Nov	−0.01285	−0.51291	0.85769
Sheridan CA Nov–Apr	−0.01716	−0.33190	0.67706
Oklahoma City OK Apr–May	−0.01034	−0.44446	0.75298
Denver CO All Year	−0.00950	−0.22866	0.56300

measurement of vapor and liquid in the zenith for the conditions of Oklahoma City, Oklahoma are shown in Fig. 6a. Note that, for cloud liquid much in excess of 3 mm, retrieval accuracies are marginal. As shown below, adaptive retrieval methods can increase the range of cloud liquid over which accurate retrievals can be obtained. However, because of the low frequency of occurrence of nonprecipitating clouds whose liquid in the zenith direction exceeds 3 mm, ordinary statistical retrieval methods are adequate most of the time.

b. *Adaptive statistical inversion*

Linear statistical inversion techniques, described in (a) of this section have led to accurate measurements of water vapor during clear conditions or during conditions of light clouds (Guiraud *et al.*, 1979). However, retrievals are not always satisfactory during periods in which clouds with high liquid content are present. To extend the range of cloud liquid under which the radiometer can operate, Westwater and Guiraud, (1980) developed an adaptive method of retrieving both vapor and liquid. The method is adaptive in the sense that the retrieval coefficients are themselves functions of the amounts of liquid and vapor that are present. For example, the relationship involved in determining vapor now becomes:

$$\hat{V} = a_0(L) + a_1(L)\tau_{20.6} + a_2(L)\tau_{31.65},$$

where the $a_i(L)$ are the adaptive coefficients. These coefficients for the climatology of Oklahoma City are shown in Figs. 6b and 6d. The behavior of the coefficients as a function of L is qualitatively explained as follows. For $L = 0$, we are solving two equations for one unknown; consequently, we derive a least squares solution with positive a_1 and a_2. For intermediate values of L, say $0.02 \leq L \leq 0.5$ cm, we are solving two equations for two unknowns, and the resulting coefficients are close to those derived by statistical inversion (see Table 3). Finally, for $L > 0.5$ cm, the effective error resulting from large liquid drives the coefficients a_1 and a_2 to zero, and the solution approaches the climatological mean. The predicted rms retrieval error for vapor as a function of liquid content is shown in Fig. 6c. This figure, compared with Fig. 6a, indicates the theoretical reduction in error achieved by the adaptive coefficient method.

In a similar manner, we can derive coefficients to infer L from τ if V is fixed. However, since the climatic variation of the vapor mass absorption coefficients is much less than that of liquid, the sensitivity to V is also much less for this case; this is seen in Fig. 6d, where the liquid retrieval coefficients are shown as a function of V.

In Section 9, examples of retrievals are given using the methods outlined above.

9. Measurements of water vapor

The integrated amount of water vapor in the zenith direction, the total precipitable water vapor (PWV), is used routinely in weather forecasting, being especially relevant to prediction of precipitation. Radiosonde soundings, made twice daily at stations of the National Weather Service (NWS), are integrated to obtain the total PWV; these are used in making long-term comparisons of PWV with the measurements of the dual-channel radiometer.

a. *Long-term measurements*

Total PWV measured by a dual-channel radiometer with amounts obtained by operational radiosondes have been compared over a six-month period at the NWS WSFO, Stapleton Airport, Denver, Colorado (Guiraud *et al.*, 1979). An analog plot of total PWV, over a two-week period, is shown in Fig. 7. The solid record is the radiometric measurement, and the triangles are total precipitable water vapor from integrated radiosonde data obtained at 12 h intervals. Of the differences that do exist on individual readings, we do not know how much is due to the radiometric system and how much is error stemming from the

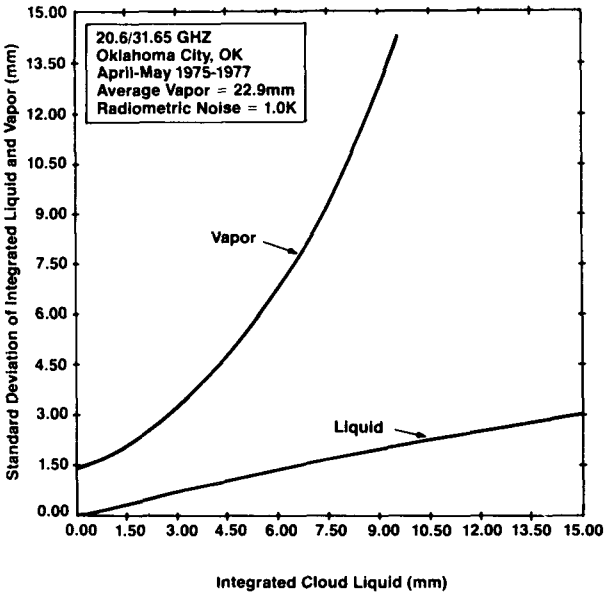

FIG. 6a. Predicted rms error in vapor and liquid retrieval from a dual-frequency radiometer as a function of cloud liquid.

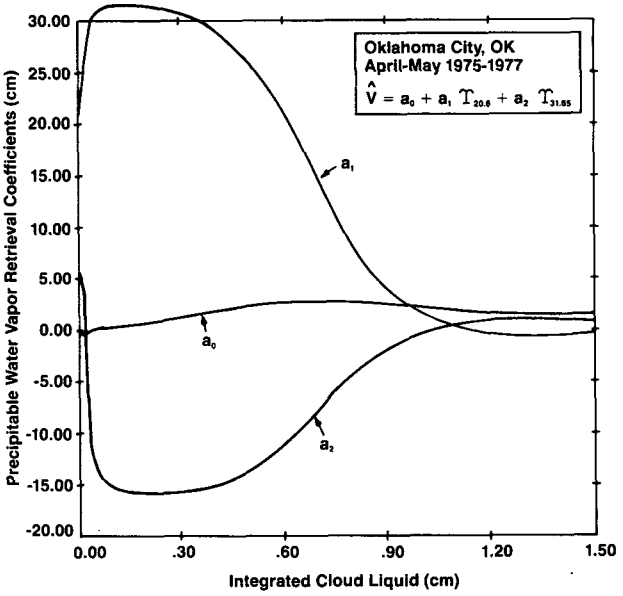

FIG. 6b. Adaptive water vapor retrieval coefficients as a function of cloud liquid.

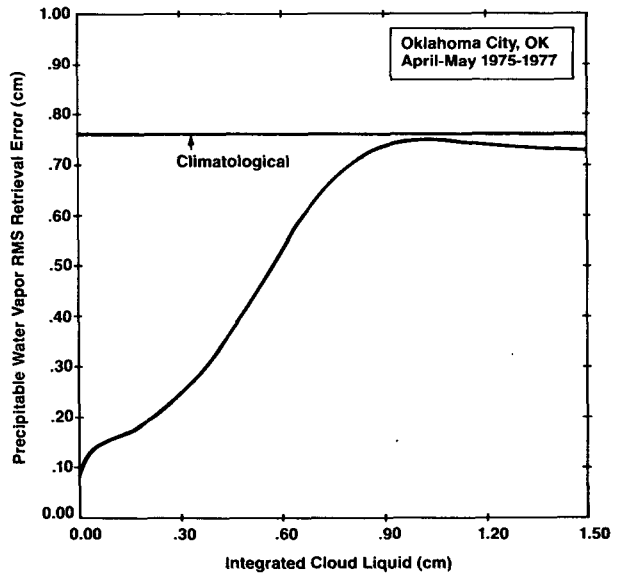

FIG. 6c. Theoretical rms error in vapor retrieval using the adaptive method.

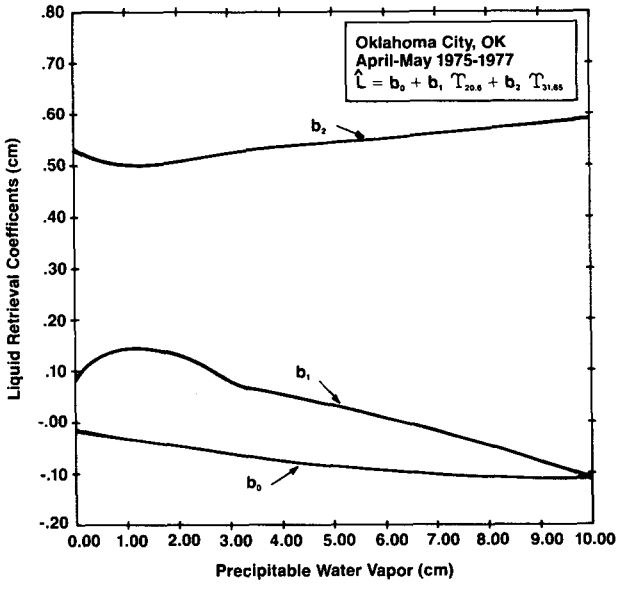

FIG. 6d. Adaptive liquid water retrieval coefficients as a function of cloud liquid.

radiosonde measurement. It is clear, however, that during certain 12 h intervals [e.g., 8 August (p.m.) to 9 August (a.m.)], a considerable amount of vapor passes overhead unobserved by the sondes.

Further insight into performance is obtained by plotting precipitable water vapor amounts measured by the radiometer, V_R, and the radiosonde directly against one another, as in Fig. 8. In a six-month sample taken at Denver (Fig. 8a), the rms difference between the two is $\Delta = 1.7$ mm, some part of this being attributable to each measuring device. A similar data set, taken over a 3-month period at Sterling, Virginia, is shown in Fig. 8b). For mid-range temperatures, the rms difference between the PWV measured by operational radiosonde, V_S, and the actual amount of vapor, V_A, is estimated to be $\delta = V_S - V_A = 1.5$ mm for Denver where the average PWV is about 1.5 cm. Assuming no correlation between radiosonde and ra-

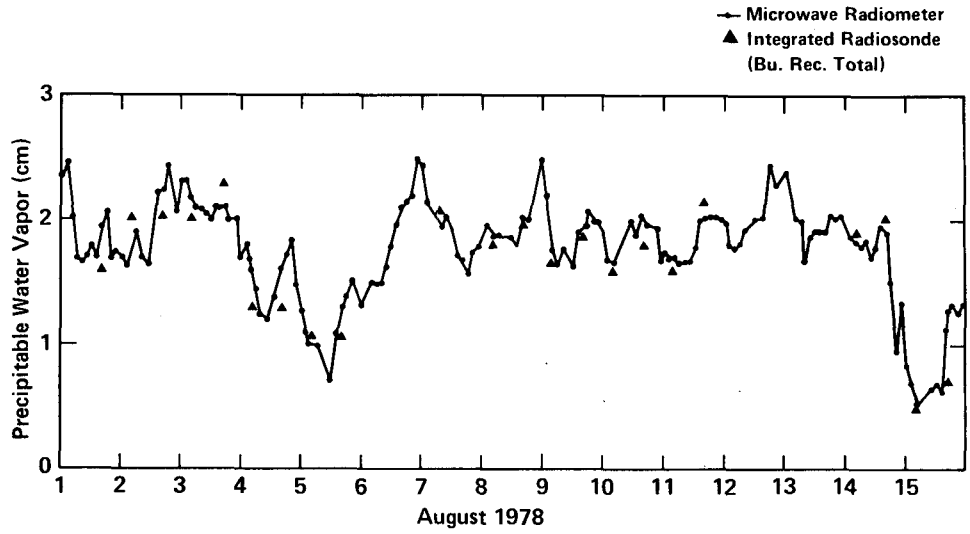

FIG. 7. Time-series of precipitable water vapor measured by dual-channel radiometry compared with amounts obtained by radiosondes at Denver, Colorado.

diometric errors, one obtains

$$\overline{(V_R - V_A)^2} = \Delta^2 - \delta^2.$$

For the Denver data set, this results in 0.8 mm for the rms error of the radiometric measurement. For the data taken at Sterling, Virginia where the average PWV is about 3.5 cm, the estimate of the rms error of operational radiosondes during average conditions is taken to be 2.1 mm. Since the measured rms radiometer/radiosonde difference is 2.6 mm at Sterling, the radiometer accuracy is estimated to be about 1.5 mm. However, all that can be said with confidence at present is that the radiometric values are about the same as, or better than, those of the radiosonde.

It should be emphasized that all data for the measurement periods, regardless of weather conditions, are plotted in Fig. 8 for those times when total precipitable water vapor from the radiosondes was available. This remark points to the fact that many cases involving clouds are included.

b. *Short-term measurements*

First evidence of the overall stability of a dual-channel system was obtained at Denver, Colorado, in December 1978, as shown in Fig. 9. The atmosphere became very dry, the precipitable water vapor decreasing from 0.5 ~0.2 cm during the early morning. Then, for an interval of about two hours, 8 to 10 a.m., the atmosphere was remarkably stable. The data over this interval, which had been recorded in the form of 2 min averages, was analyzed; a rms deviation of 0.007 cm was obtained.

It is possible to determine the magnitude of the vapor fluctuations and their associated periods by way of spectral analysis (Hogg *et al.*, 1981). The amount of water vapor varies greatly with time. For synoptic weather forecasting, one obtains this quantity by integrating *in situ* measurements from balloon-borne radiosondes conventionally launched every 12 h; but the periodicities of the variations span a wide scale. Weather fronts and other phenomena give rise to variations on the order of hours. In addition, there are cloud-sized patches of vapor that produce fluctuations with periods of minutes, as well as very small-scale patches, caused by turbulence, that move with the wind and can give rise to periods on the order of seconds.

Fig. 10 is a time series showing how the PWV varies during a time interval of a few days. On day 273, for example, the PWV decreased to half-value from midnight to midday, and then regained half of that decrease by evening. Periods of much less than an hour are evident in the fine-grained low amplitude fluctuations near noon of day 269. The time constant of the instrument is 2 min for these data.

Examples of spectra are shown in Fig. 11; curve (a) corresponds to the time series of Fig. 10. The length of the individual data samples was 34 hours, and five of these were averaged to produce the spectrum of curve (a). The weather was clear with broken clouds; the average PWV for the period was about 1.2 cm, and the average wind was about 8 m s^{-1}. Another spectrum, taken under much drier conditions, is curve (b) in Fig. 11; three 34 h data samples were averaged.

A matter of considerable interest in the theory of atmospheric structure is the slope of the power spectrum. Although we have found the shape to change considerably with weather conditions, one can fit the slopes of spectra such as those in Fig. 11 with relationships of the form $S(F) = KF^{-x}$. However, it is

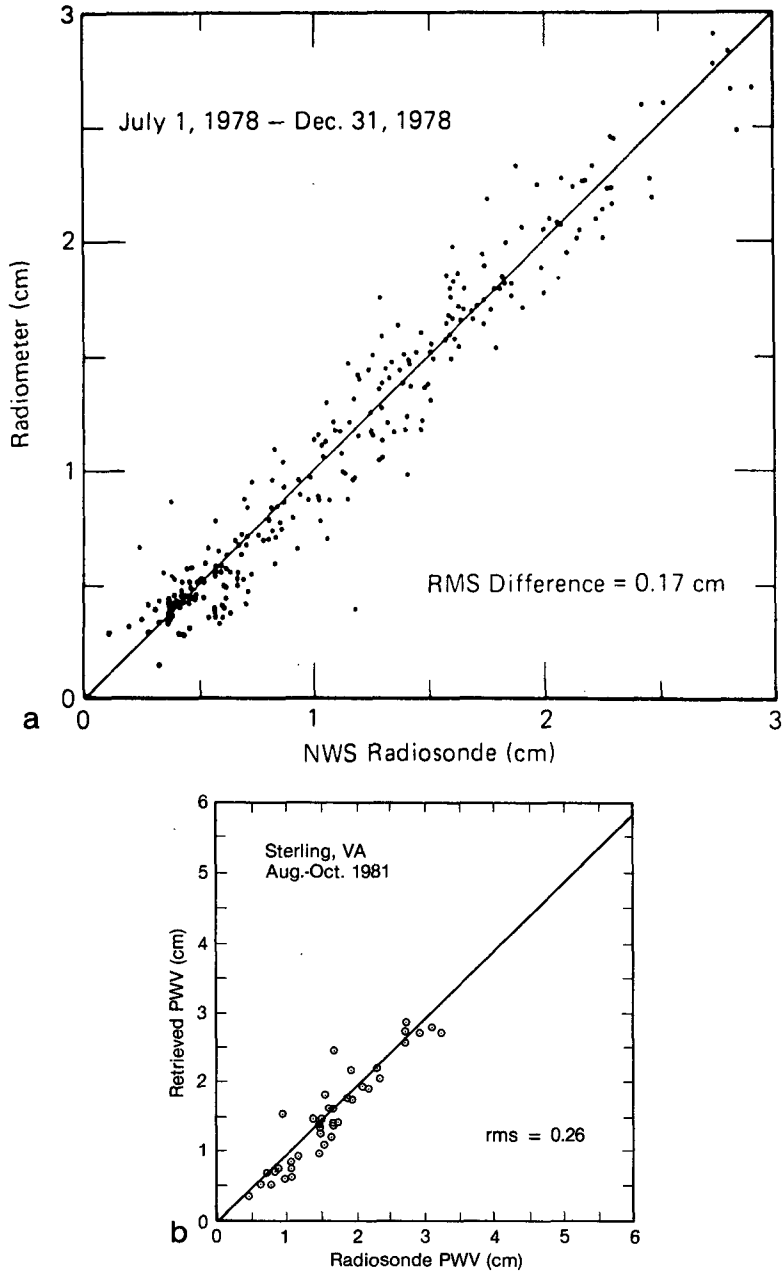

FIG. 8a. Plot showing the differences between precipitable water vapor measured by dual-channel radiometer and radiosonde during a 6-month period at Denver, Colorado. (b) A similar set measured at Sterling, Virginia, August through October 1981.

clear from Fig. 11 that the curves can be more satisfactorily represented by two straight lines rather than by one. Such being the case, the behavior of the PWV spectrum appears to change at about $F = 10$, corresponding to a period of about 2.5 hours.

c. Other comparative measurements

Another way of establishing the credibility of an instrument of given design is to construct two of them and compare the measured data from the two instruments in the same environment. Such a comparison was made during part of the summer of 1981 between two dual-channel radiometers, with vertically-oriented beams, situated side-by-side at Denver, Colorado. Fig. 12 shows a plot of precipitable water vapor measured by the two dual-channel radiometers, one as ordinate and the other as abscissa. The points are 2-min averages. The root-mean-square difference

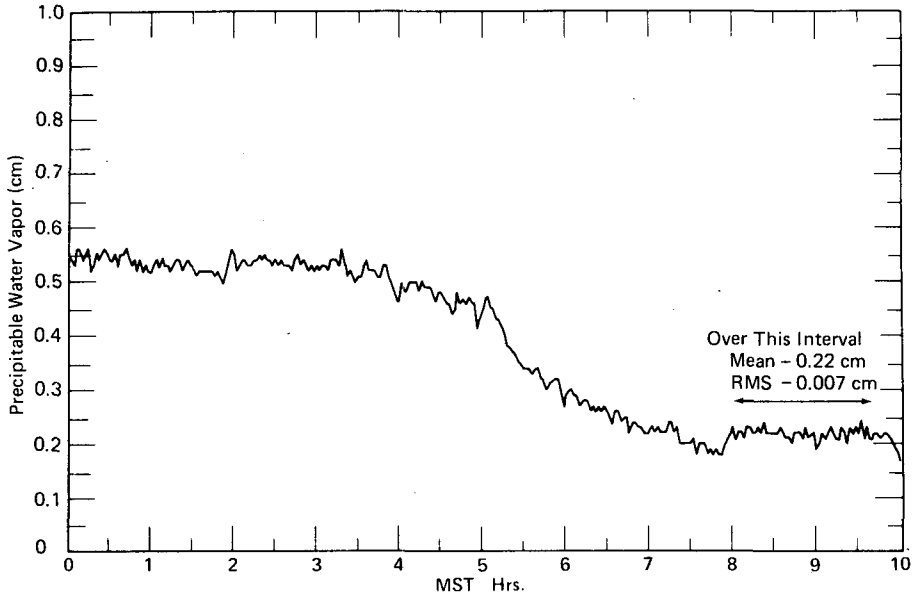

FIG. 9. Radiometrically measured total-precipitable water vapor at Denver, Colorado, WSFO, 13 December 1978; the measurements are 2-minute averages on a clear, very dry day.

between the two sets is about 0.8 mm, the same number as obtained by the estimate discussed in (a) of this section in connection with the data of Fig. 8. Clearly, the two instruments measure the same amount of water vapor.

If the atmosphere happens to be horizontally homogeneous, and if the radiometric instrument is properly leveled, the radiometer, with the antenna beam at a fixed elevation angle, should produce a constant output over a full rotation in azimuth. Under the above assumptions, the constancy of the output is some measure of the quality of the antenna radiation pattern, especially when the elevation is low. Fig. 13 shows three azimuth scans, with elevation angle 20°, taken near Auburn, California, on 10 March 1981; each rotation is completed in about 20 min. The integrated vapor is about 3.5 cm at all azimuths, a fairly dry day, with corresponding PWV of 1.2 cm; the 3.5 cm value appears to be well preserved over the one-hour period of measurement.

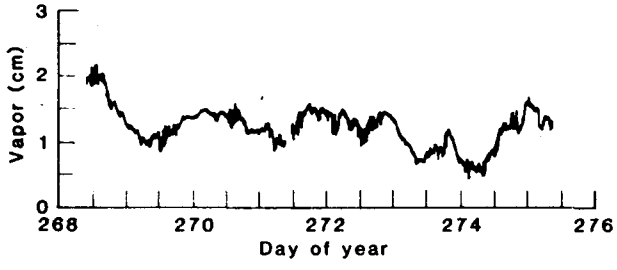

FIG. 10. Microwave radiometric measurement of total PWV for a 7-day period at the Weather Service Forecasting Office, Denver, Colorado.

This behavior is, however, by no means typical; the integrated vapor can be distributed in various fashions as a function of azimuth.

Gross profiling of water vapor can be achieved by a dual-channel radiometer in conjunction with surface measurements of humidity. Surface measurements of temperature and pressure are also beneficial in the profiling process. The method used in retrieving these profiles is discussed in detail by Westwater *et al.* (1983) and is also referred to in a companion paper in this issue (Hogg *et al.*, 1983). Similar work has been started in Sweden (Skoog *et al.*, 1982). An example of a vapor profile using this type of system is shown in Fig. 14.

d. Comparison of retrievals using statistical and adaptive-statistical methods

A dual-channel radiometer was operated at Lawton (Fort Sill), Oklahoma as part of a Severe Storms and Mesoscale Experiment (SESAME). The radiometer was located there to provide a continuous monitor of total precipitable vapor as it flowed from the Gulf of Mexico into the SESAME monitoring area. There were many periods during which clouds with high liquid content were present; frequently these conditions developed into severe storms and rain. Retrievals of vapor during these high-liquid conditions were performed, using both statistical (Section 8a) and adaptive statistical methods (Section 8b) because of the high likelihood of heavy rain. We did not attempt to retrieve vapor when the 30 GHz brightness temperature exceeded 250 K.

We present data on a case study of a 7-day period

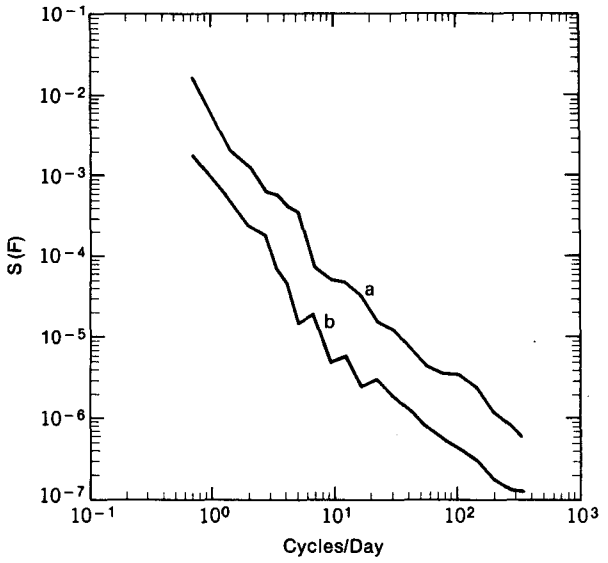

FIG. 11. Curve (a) is the spectrum of the PWV of Fig. 10, averaged over five 34-hour periods; the average PWV for the period is 1.2 cm. Curve (b) is the corresponding spectrum for a drier condition over three 34-hour periods; the average PWV is 0.35 cm. The units of the ordinate are square centimeters per cycle per day.

for which 1) there were periods of high liquid content and 2) the Fort Sill and the Oklahoma City soundings were in reasonable agreement. The case selected is shown in Figs. 15a, b, in which nonadaptive statistical and adaptive retrievals are shown. During periods of high liquid the adaptive retrieval yields vapor estimates substantially lower than those of the nonadaptive method, but the retrievals are practically identical during periods of clear to low liquid content. In all likelihood, the vapor estimates during times of high liquid, such as the spikes of liquid greater than ~1 cm, exceed the true value.

10. Measurement of liquid

Interest in the amounts of liquid measured by dual-channel radiometry was sparked by observations of super-cooled liquid that were directly associated with icing of aircraft (Hogg *et al.*, 1980a). The interest stemmed primarily from the weather-modification community for whom the amount of liquid in winter clouds is an important parameter. However, there was no direct evidence of the accuracy of the amount measured due, as mentioned in the introduction, to lack of an independent method of measuring the liquid routinely. An independent measuring system based upon *transmission* of a millimeter-wave signal from the COMSTAR satellite was therefore implemented (Snider *et al.*, 1980a). Long-term side-by-side comparisons of the amount of liquid in clouds were made with this system and a dual-channel radiometer (Snider *et al.*, 1980b). The results of these measurements are shown in Fig. 16 where the amount of liquid measured by the dual-channel radiometer is the ordinate and by the satellite transmission system,

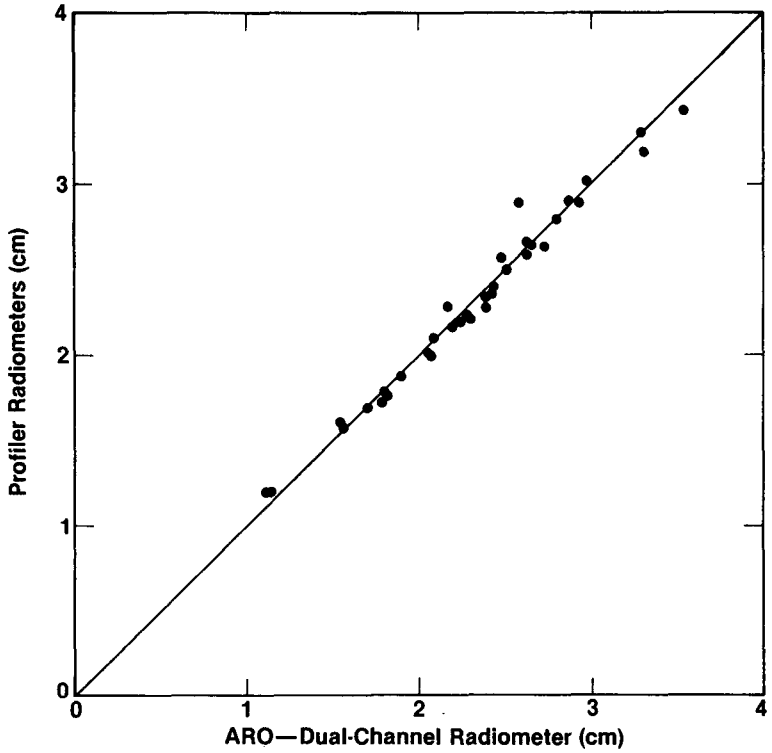

FIG. 12. Side-by-side measurements of precipitable water vapor by two dual-channel radiometers; Stapleton Airport, Denver, Colorado, 15 June–16 July 1981.

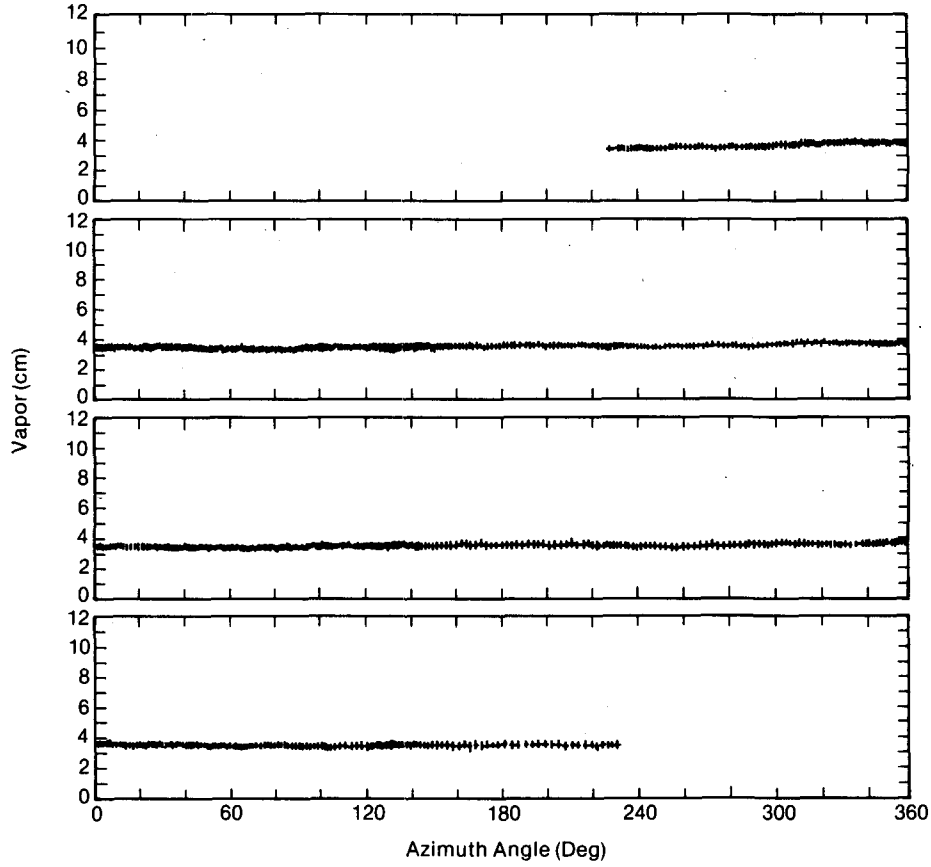

FIG. 13. Azimuthal scans showing integrated water vapor on slant paths at an elevation of 20° during a day when the atmosphere was quite homogeneous; Auburn, California, 10 March 1981.

the abscissa. Although the filling of the antenna beams (by clouds) is not the same in the two systems, these comparisons lend confidence that dual-channel radiometers indeed measure the integrated amount of cloud liquid quite well.

The steerable dual-channel radiometer has been employed in weather-modification studies during the winter months (Rauber *et al.*, 1982). It is of interest that the instrument can be unattended in some modes of operation, and operated by someone given minimal instruction for special modes. Examples of azimuth scans (elevation angle 12.5°) showing the liquid-bearing clouds approaching from the west are given in Fig. 17, along with the integrated vapor on the slant path. In this case, the scans are taken over a period of about 20 minutes. As presently configured, the instrument measures the integrated amount of liquid with a sensitivity of about 0.1 mm. In Fig. 17, the integrated vapor is about the same, 6.5 cm, at all azimuths during the four scans. But the clouds, with peak amounts of integrated liquid of about 4 mm; move from the west, over the site, toward the east (as indicated on the fourth scan) during the one and a half hour period.

11. Applications

a. Forecasting of weather

The relevance of observations made by dual-channel radiometers to weather forecasting is discussed in some detail in a companion paper (Hogg *et al.*, 1983), therefore only a brief discussion will be given here.

An example of some early data measured by a dual-channel radiometer in the zenith-pointing configuration at Lawton, Oklahoma (Westwater and Guiraud, 1980), is shown in Fig. 18; this is a typical example of behavior over a period of about a week in early summer. Beginning with day 132, the amount of water vapor overhead is low (less than 1 cm of equivalent liquid), i.e., the weather is dry. But a gradual increase in vapor takes place, and liquid-bearing clouds appear on day 138. Further increase in vapor to about 4 cm results in a heavy rain of rate 80 mm h^{-1} on day 140. It is data such as these that are believed applicable in improving mesoscale weather-prediction.

Note in Fig. 18, during the interval on day 140 when the 80 mm h^{-1} rain occurred, that the radiometer saturates due to excessive radiation. The ab-

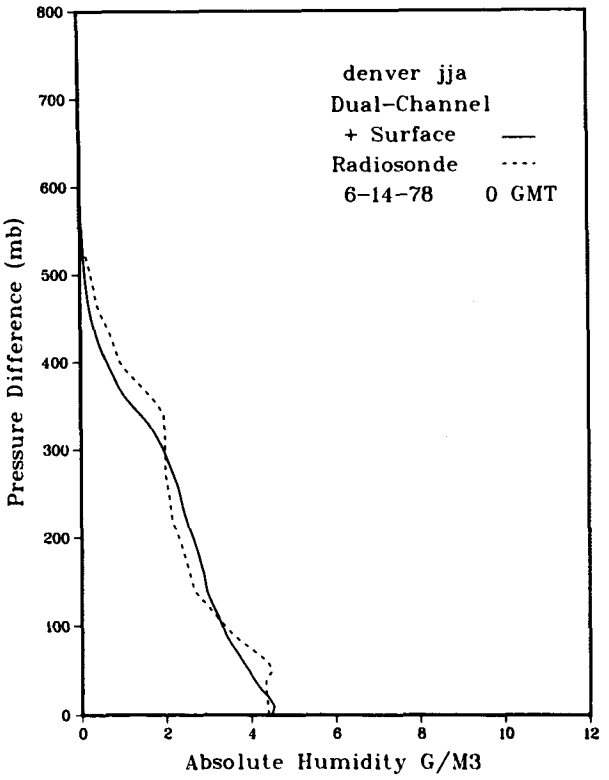

FIG. 14. A humidity profile computed for dual-channel radiometric and surface data compared with radiosonde profile.

sorption (and therefore emission) from the liquid is so high that the retrieved vapor is in accurate during that interval of time. Operationally, a threshold on the amount of liquid permitted for a required accuracy in vapor can be applied; for liquid above the threshold, the data are rejected. The application of algorithms based upon adaptive retrieval coefficients (Section 8b) can be implemented to alleviate this behavior somewhat.

b. *Weather-modification experiments*

The first long-term application of microwave radiometers in weather-modification studies was, to the best of our knowledge, by the Bureau of Reclamation of the U.S. Department of the Interior, by the State University of Utah and by the Colorado State University. The first and last of these organizations employed a fully-steerable unit built by the Wave Propagation Laboratory for the Army Research Office. Utah State University constructed their own instrument, with the antenna beam scannable in the elevation plane only, following the original design of Guiraud *et al.* (1979).

The exterior component of the antenna system in both cases is a 45° flat reflector, as mentioned in Section 4. The effect of rain wetting this reflector is known, by local spraying tests, to have little effect on overall operation. Likewise, dry snow on the reflector is not troublesome since frozen water has negligible loss, and only the phase of the electromagnetic waves is somewhat perturbed (thereby modifying the antenna radiation pattern somewhat). However, wet snow that adheres to the flat reflector can cause serious errors in both the vapor and liquid determinations. The only practical way of overcoming this problem (known to us) is generation of an automatically initiated air-flow over the reflector by means of a fan, or jet, thereby preventing the wet snow from reaching the reflector. Tests on this technique have been made at the State University of Utah and at the Wave Propagation Laboratory.

Measurements of super-cooled liquid and vapor taken by radiometers during weather-modification exercises have been successful (Snider and Rottner, 1982), but these will be discussed in depth in future publications. Utility of the data appears to be high as an indicator for initiation of seeding, and in relationship to formulation of realistic cloud models, especially in the vicinity of mountain ranges.

c. *Very long baseline interferometry and geodetic metrology*

Since variations in the amount of water vapor along a path through the atmosphere are the prime cause of variations in the phase of a radio wave propagated along that path, the dual-channel radiometer is useful in systems designed to measure crustal motion of the earth accurately. The short-term variations in vapor are illustrated by the spectra shown in Fig. 11. The excess path length encountered by the radio wave due to the vapor, is $L_v = 6.5V$ where both L_v and V are in the same units, say cm, V being the integrated vapor along the path. With the high stability achieved by the dual-channel instrument in measurement of vapor, it is estimated that the excess path length L_v, can be determined to about 0.5 cm for long-term operation (Hogg *et al.*, 1980b). Corrections to this order of accuracy are of value in geodetic surveying (MacDoran, 1979), and in related measurement systems such as the Global Positioning System. Dual-channel radiometers for this purpose have also been designed and implemented by the Jet Propulsion Laboratory and several other organizations have units of the type discussed in this paper under construction.

Experience has shown that the long-term variations in path-integrated vapor are large enough to produce changes in excess radio path-length of tens of centimeters, amounts sufficient to limit significantly performance of the precise surveying systems mentioned above. Real-time corrections for these varying path lengths can significantly improve the resolution of these interferometric systems.

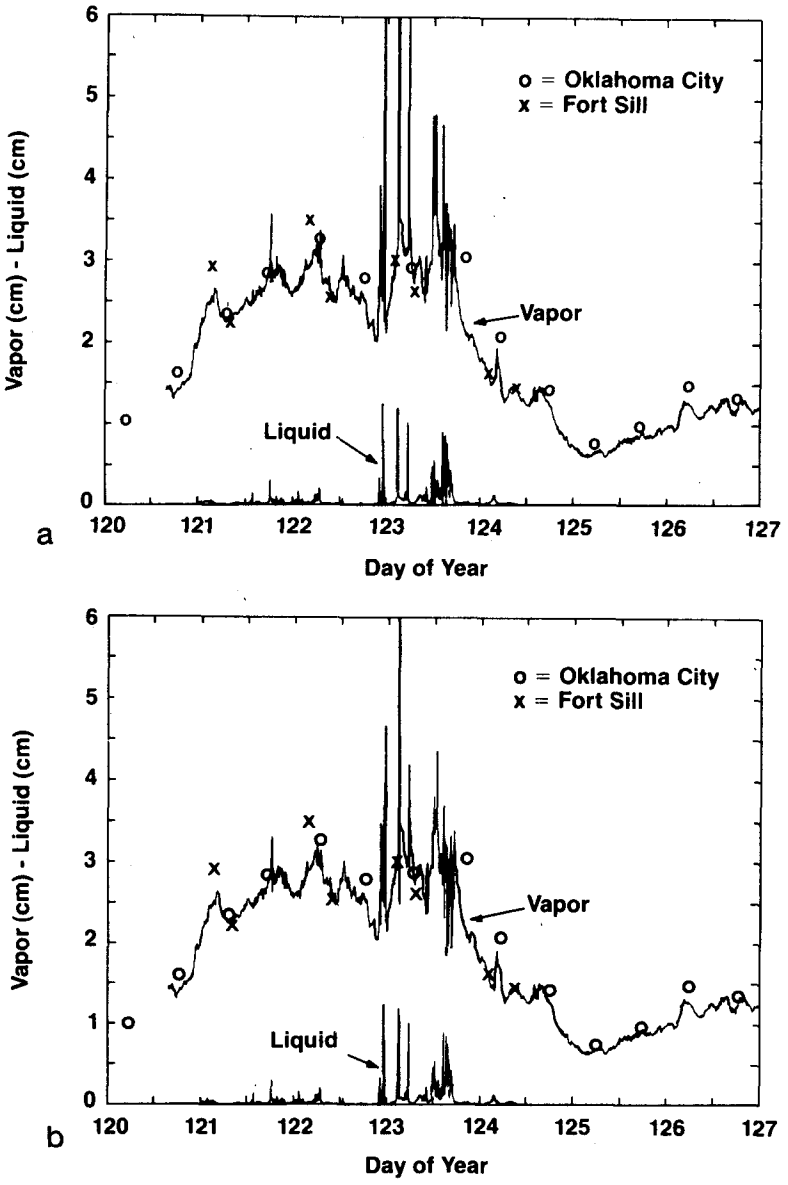

FIG. 15a. Nonadaptive statistical retrieval of vapor and liquid. Data were taken on 30 April–7 May 1979, during SESAME experiment. (b) Adaptive retrieval of vapor and liquid.

d. Research on solar radiation through clouds, and hurricane studies

Measurements of both liquid in clouds and the amount of vapor in the troposphere are of interest in determining the amount of solar radiation reaching the surface of the earth. The liquid is believed to attenuate the radiation more strongly than the ice in clouds (Platt, 1981). Thus experiments utilizing microwave dual-channel radiometers in conjunction with pyranometers are expected to be performed in the near future. This work is related to studies of climate.

The amount of liquid above the zero-degree isotherm is a useful parameter in the study of hurricanes. Although the amount of vapor above that level can sometimes be estimated by other means, a dual-channel (rather than single-channel) instrument is preferable because the liquid and vapor are separately measured, and ambiguity as to the amount of liquid is obviated.

In these two research applications, it is mandatory that the instruments be mountable on aircraft since, in the case of the solar studies, observations are also often taken over the oceans. Preferably, the configuration for the antenna on an aircraft would be sim-

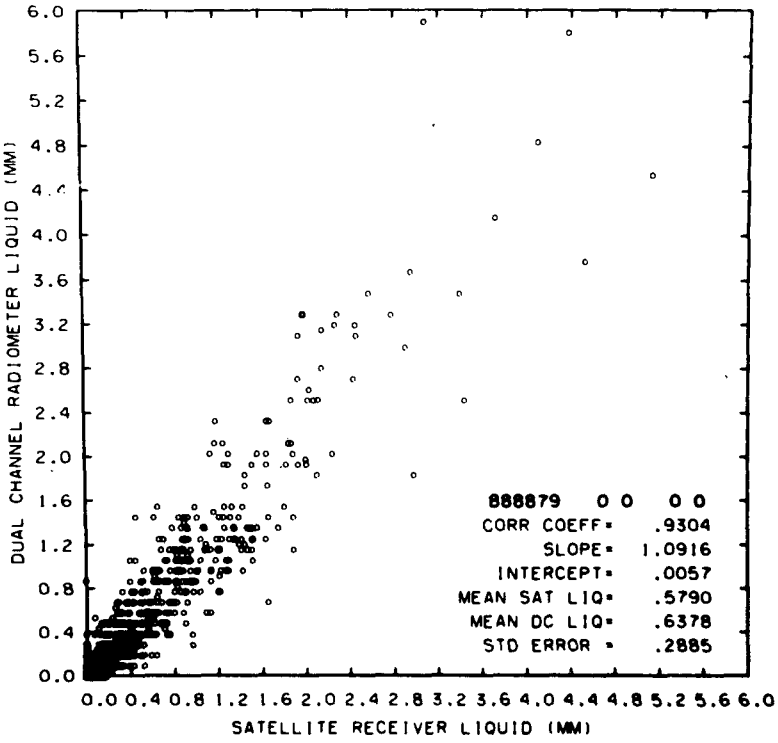

FIG. 16. Comparison of cloud liquid measured by dual-channel radiometer (ordinate) and satellite receiver (abscissa). Measurements were made during August 1979 at the National Weather Service Forecast Office, Denver, Colorado.

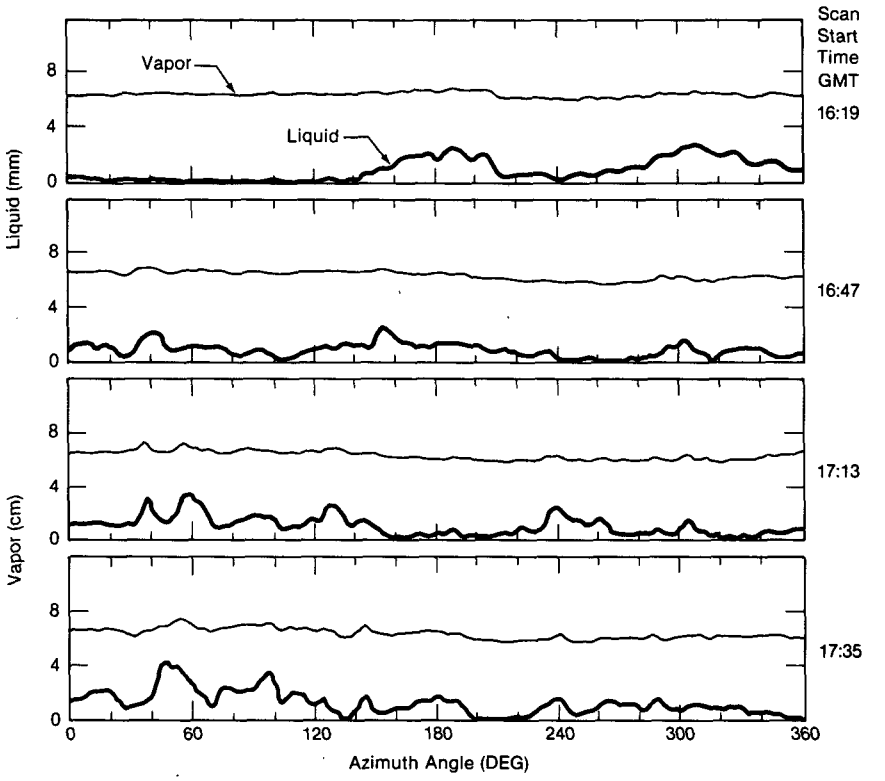

FIG. 17. Azimuth scans, with the antenna beam at an elevation angle of 12.5°, showing progression of liquid-bearing clouds from west to east; taken on 1 April 1981 with the instrument located in California, west of the Sierra mountains.

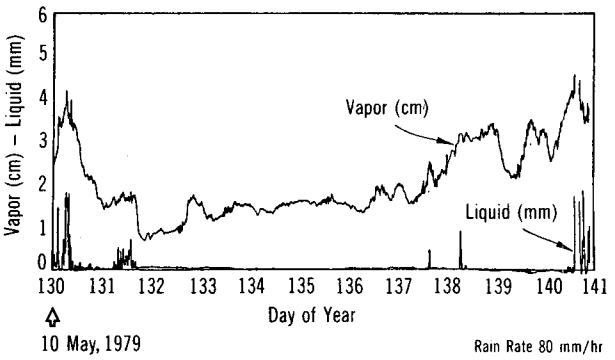

FIG. 18. An 8-day buildup of precipitable water vapor resulting in high liquid content in clouds, and finally, heavy rainfall.

ilar to the design in which the beam is scannable only in the elevation plane (Guiraud *et al.*, 1979). The antenna elements would be about half the size of those in the ground-based model, and the flat reflector, about 30 cm in dimension, would preferably be mounted on the side of the aircraft. The half-power beamwidth of the radiation pattern would be about 6°, the beam being pointable toward the zenith or at any angle from zenith forward to the line of flight. In this configuration, elevation scans, similar to those discussed in Section 7, can be made if any calibration is required.

Acknowledgments. Funding for construction of the prototype fully steerable dual-channel radiometer was supplied in part by the U.S. Army Research Office, Contract 1L161102BH57-01, and for operations, by the Bureau of Reclamation of the U.S. Department of the Interior, and by the Wave Propagation Laboratory (WPL), ERL, NOAA, DOC; we especially thank H. M. Burdick of WPL for his help in both the constructional and operational phases of the work, and R. J. Stone of the Test and Evaluation Division of the National Weather Service for help with the measurements at the NWS site in Virginia.

REFERENCES

Decker, M. T., E. R. Westwater and F. O. Guiraud, 1978: Experimental evaluation of ground-based microwave radiometric sensing of atmospheric temperature and water vapor profiles. *J. Appl. Meteor.*, **17**, 1788–1795.

Deepak, A., 1980: *Atmospheric Water Vapor,* A. Deepak, T. D. Wilkerson and L. H. Ruhnke, Eds. Academic Press.

Deutsch, R., 1965: *Estimation Theory.* Prentice-Hall, 54–71.

Gaut, N. E., and E. C. Reifenstein, III, 1971: Interaction model of microwave energy and atmospheric variables. Environ. Res. Tech., Rep. No. 13.

Grody, N. C., A. Gruber and W. C. Shen, 1980: Atmospheric water content over the tropical Pacific derived from the Nimbus-6 scanning microwave spectrometer. *J. Appl. Meteor.*, **19**, 986–996.

Guiraud, F. O., J. Howard and D. C. Hogg, 1979: A dual-channel microwave radiometer for measurement of precipitable water vapor and liquid. *IEEE Trans. Geosci. Electron.*, **GE-17**, 129–136.

Hogg, D. C., 1959: Effective antenna temperature due to oxygen and water vapor in the atmosphere. *J. Appl. Phys.*, **30**, 1417–1419.

——, and T. S. Chu, 1975: The role of rain in satellite communications. *Proc. IEEE,* **63**, 1308–1331.

——, F. O. Guiraud and E. B. Burton, 1980a: Simultaneous observation of cool cloud liquid by ground-based microwave radiometry and icing of aircraft. *J. Appl. Meteor.*, **19**, 893–895.

——, —— and M. T. Decker, 1980b: Measurement of excess ratio transmission length on earth-space paths. *Astron. Astrophys.*, **95**, 304–307.

——, ——, J. Howard, A. C. Newell, D. P. Kremer and A. G. Repjar, 1979: An antenna for dual-wavelength radiometry at 21 and 32 GHz. *IEEE Trans. Antennas Propag.*, **AP-27**, 764–771.

——, —— and W. B. Sweezy, 1981: The short-term temporal spectrum of precipitable water vapor. *Science,* **213**, 1112–1113.

——, ——, J. B. Snider, M. T. Decker and E. R. Westwater, 1982: Microwave radiometry for measurement of water vapor.

——, M. T. Decker, F. O. Guiraud, K. B. Earnshaw, D. A. Merritt, K. P. Moran, W. B. Sweezy, R. G. Strauch, E. R. Westwater and C. G. Little, 1983: An automatic profiler of the temperature, wind, and humidity in the troposphere. *J. Climate Appl. Meteor.*, **22**, 807–831.

Platt, C. M. R., 1981: Extended clouds and radiation. World Climate Research Programme, **18**, Vol. 18, WMO, 1–37.

Rauber, R. M., J. B. Snider and L. O. Grant, 1982: Spatial variations of cloud liquid water determined by aircraft and microwave radiometer measurements in northern Colorado orographic storms. *Proc. Conf. Cloud Physics,* Chicago, Amer. Meteor. Soc., 477–480.

Skoog, B. G., J. I. H. Askne and G. Elgered, 1982: Experimental determination of water vapor profiles from ground-based radiometer measurements at 21.0 and 31.4 GHz. *J. Appl. Meteor.*, **21**, 394–400.

Snider, J. B., and D. Rottner, 1982: The use of microwave radiometry to determine a cloud seeding opportunity. *J. Appl. Meteor.*, **21**, 1286–1291.

——, H. M. Burdick and D. C. Hogg, 1980a: Cloud liquid measurement with a ground-based microwave instrument. *Radio Sci.*, **15**, 683–693.

——, F. O. Guiraud and D. C. Hogg, 1980b: Comparison of cloud liquid content measured by two independent ground-based systems. *J. Appl. Meteor.*, **19**, 577–579.

Staelin, D. H., 1966: Measurements and interpretation of the microwave spectrum of the terrestrial atmosphere near 1 centimeter wavelength. *J. Geophys.*, **71**, 2875–2881.

——, A. L. Cassel, K. F. Kunzi, R. L. Pettyjohn, R. K. L. Poon and P. W. Rosenkranz, 1975: Microwave atmospheric temperature sounding: Effects of clouds on the Nimbus-5 satellite data. *J. Atmos. Sci.*, **32**, 1970–1976.

——, K. F. Kunzi, R. L. Pettyjohn, R. K. L. Poon, R. W. Wilcox and J. W. Waters, 1976: Remote sensing of atmospheric water vapor and liquid water with the Nimbus-5 microwave spectrometer. *J. Appl. Meteor.*, **15**, 1204–1214.

Westwater, E. R., 1967: An analysis of the correction of ray errors due to atmospheric refraction by microwave radiometric techniques. ESSA Tech. Rep. IER 30-ITSA 30.

——, 1978: The accuracy of water vapor and cloud liquid determination by dual frequency ground-based microwave radiometry. *Radio Sci.*, **13**, 677–685.

——, and F. O. Guiraud, 1980: Ground-based microwave radiometric retrieval of precipitable water vapor in the presence of clouds with high liquid content. *Radio Sci.*, **15**, 947–957.

——, M. J. Falls and D. C. Hogg, 1983: Dual-channel microwave radiometric remote sensing of water vapor profiles. To be submitted to *J. Climate Appl. Meteor.*